Article

Competitive Hydrogen Atom Transfer to Oxyl- and Peroxyl Radicals in the Cu-Catalyzed Oxidative Coupling of N-Aryl Tetrahydroisoquinolines Using tert-Butyl Hydroperoxide

Esther Böß, Larry Michael Wolf, Santanu Malakar, Michela Salamone, Massimo Bietti, Walter Thiel, and Martin Klussmann

ACS Catal., **Just Accepted Manuscript** • DOI: 10.1021/acscatal.6b00944 • Publication Date (Web): 11 Apr 2016

Competitive Hydrogen Atom Transfer to Oxyl- and Peroxyl Radicals in the Cu-Catalyzed Oxidative Coupling of *N*-Aryl Tetrahydroisoquinolines Using *tert*-Butyl Hydroperoxide

Esther Boess,[†] Larry M. Wolf,[†] Santanu Malakar,[†,§] Michela Salamone,[‡] Massimo Bietti,*[,‡] Walter Thiel*[,†] and Martin Klussmann*[,†]

[†]Max-Planck-Institut für Kohlenforschung, Kaiser-Wilhelm-Platz 1, 45470 Mülheim an der Ruhr, Germany

[‡]Dipartimento di Scienze e Tecnologie Chimiche Università "Tor Vergata", Via della Ricerca Scientifica 1, 00133 Rome, Italy

[§]Present address: Department of Chemistry, Indian Institute of Technology Bombay, Powai, Mumbai 400076, India

ABSTRACT: The question of whether hydrogen atom transfer (HAT) or electron transfer (ET) is the key step in the activation of *N*-aryl tetrahydroisoquinolines in oxidative coupling reactions using CuBr as catalyst and *tert*-butyl hydroperoxide (*t*BuOOH) has been investigated. Strong indications for a HAT mechanism were derived by using different *para*-substituted *N*-aryl tetrahydroisoquinolines, showing that electronic effects play a minor role in the reaction. Hammett plots of the Cu-catalyzed reaction, a direct time-resolved kinetic study with *in situ* generated cumyloxyl radicals, as well as density functional calculations gave essentially the same results. We conclude from these results and from kinetic isotope effect experiments that HAT is mostly mediated by *tert*-butoxyl radicals and only to a lesser extent by *tert*-butylperoxyl radicals, in contrast to common assumptions. However, reaction conditions affect the competition between these two pathways, which can significantly change the magnitude of kinetic isotope effects.

KEYWORDS: oxidative coupling, C-H functionalization, radicals, reaction mechanism, hydrogen atom transfer, kinetics, kinetic isotope effect

INTRODUCTION

Considerable attention has been devoted to oxidative cross-coupling reactions, also called cross-dehydrogenative coupling (CDC), which generate a new C-C or C-heteroatom bond from C-H and C-heteroatom bonds, respectively.[1] Among the multitude of reactions developed in recent years, especially the use of *N*-aryltetrahydroisoquinolines (**1**, *N*-aryl THIQs) or *N,N*-dimethylanilines (**2**) as substrates in coupling reactions with nucleophiles have inspired many research groups (Scheme 1a).[2] Since the first reports by Miura and Murahashi using Fe- and Ru-catalysts,[3] an increasing number of catalysts, oxidants and nucleophiles has been discovered for this type of reaction.[4,5] Most inspiring have been the reports by the group of Chao-Jun Li which used the combination of CuBr as catalyst together with *tert*-butyl hydroperoxide (*t*BuOOH) in decane as oxidant to couple **1** with a large variety of compounds to products of type **3** (Scheme 1b).[6] A few dedicated mechanistic investigations of this or closely related reactions have been reported, including a computational study.[7] However, some debate still exists over the exact mode of activation of the amine. Here we present results from kinetic and theoretical studies addressing this question.

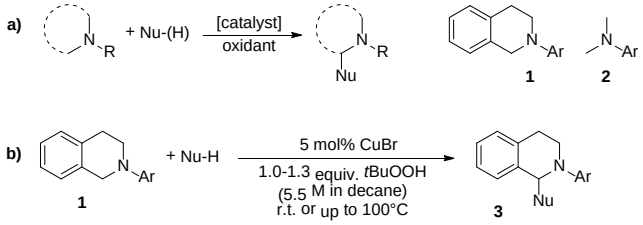

Scheme 1. a) Oxidative Coupling Reactions with Amines. b) Coupling of *N*-Aryl Tetrahydroisoquinolines with Nucleophiles using CuBr as Catalyst and *tert*-Butyl Hydroperoxide as Oxidant

It is generally assumed that CuBr, as well as several other transition metal salts and also iodide, act as catalysts to decompose *tert*-butylhydroperoxide into *tert*-butoxyl (*t*BuO•) and *tert*-butylperoxyl radicals (*t*BuOO•) (Scheme 2).[7b,7c,8] The nowadays common way of depicting this reaction is based on proposals from Kharasch, Kochi and Minisci.[8a,8b,9,10] Kochi suggested the formation of a copper peroxide complex **4** but could not rule out the involvement of free *t*BuOO•.[9b] Based on measurements of very fast hydrogen atom transfer (HAT) rates for reactions between

alkoxyl radicals and *t*BuOOH,[11] Minisci suggested that *t*BuO• formed by reaction of *t*BuOOH and Cu(I) rapidly generates *t*BuOO• in the presence of *t*BuOOH.[8b] The mechanism depicted in Scheme 2 thus illustrates the common assumption that the key intermediate in such reactions with *t*BuOOH is *t*BuOO•.

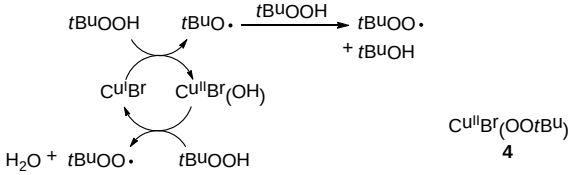

Scheme 2. CuBr-catalyzed Generation of Oxyl and Peroxyl Radicals from *tert*-Butylhydroperoxide

Oxidative coupling reactions of tertiary amines in general are supposed to proceed via electrophilic iminium ions **5** (Scheme 3a). With *N*-aryl THIQs, these have been characterized for reactions using DDQ as oxidant and $CuCl_2$ as catalyst together with oxygen, respectively.[12] Substrate studies led to the conclusion that the role of catalyst and oxidant is chiefly to form the electrophile, and the nucleophile scope is thus limited to those of sufficient reactivity to attack the iminium ion.[7b]

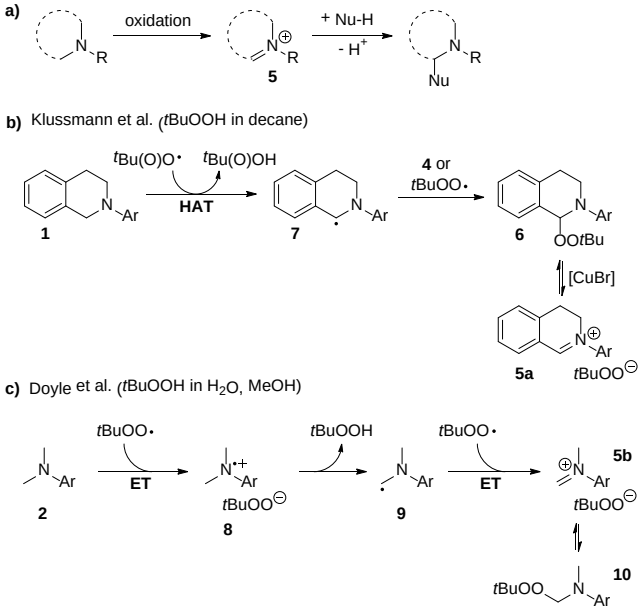

Scheme 3. a) Supposed General Mechanism for Oxidative Coupling Reactions with Amines. b), c) Suggested Oxidative Pathways in the Formation of Iminium Ions from Amines

Regarding the question of how the iminium ion intermediate is formed, we had previously suggested the formation of the observable peroxide intermediate **6** as direct precursor of iminium ion **5a** (Scheme 3b).[7b] HAT from *N*-aryl THIQ **1** to *t*BuO• or *t*BuOO• would produce the stabilized carbon radical **7**. Peroxide **6** would then be formed by radical recombination with *t*BuOO• or by peroxyl transfer from a complex like **4**. This radical pathway would thus proceed without competition by nucleophiles, which we took as explanation for the observed formation of **6** in larger amounts than any product **3** in the early stages of the reaction, regardless of the nucleophile's reactivity.[7b] The iminium ion **5a** would then be formed by reversible heterolytic C-O bond cleavage, assisted by the Lewis-acidic catalyst. Under reaction conditions, the equilibrium favors **6** and **5a** could not be detected by NMR, unless acid was added.

Ratnikov and Doyle later proposed a different mechanism for such reactions.[7c] They had investigated a Rh-catalyzed oxidative coupling reaction with *N,N*-dimethylanilines (**2**) in methanol, using aqueous *t*BuOOH as oxidant, but also explored the use of CuBr and other metal catalysts. They suggested that the initial reaction between **2** and *t*BuOO• would be electron transfer (ET), furnishing the ammoniumyl radical cation **8** and *tert*-butylperoxylate (Scheme 3c). The latter would abstract a proton from the acidified α-CH_2 bonds, resulting in carbon radical **9**, which would then generate the iminium ion **5b** by another ET to a second *t*BuOO•. The observed peroxide **10** would thus form by nucleophilic attack on the iminium ion, in competition with other nucleophiles present, including the solvent.

The key difference to our proposal, ET instead of HAT, was mainly rationalized by several kinetic isotope effect experiments and by a significant decrease in rate upon introducing electron-withdrawing substituents into the arene ring.[7c] A slope of –0.76 in a Hammett plot versus σ^+ indicated the development of a positive charge.[13] While these conclusions by Ratnikov and Doyle were convincing, they had studied a somewhat different system. We therefore felt challenged to find out whether our proposal was right or wrong by distinguishing between the possible pathways via HAT and ET, respectively.

RESULTS AND DISCUSSION

We decided to study exclusively the oxidation of amines **1** in the absence of nucleophiles to avoid complications in the kinetics and analysis, and thus investigated the formation of peroxide **6** (Scheme 4).

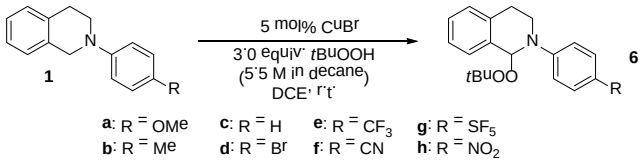

Scheme 4. Oxidation of *N*-Aryl Tetrahydroisoquinolines 1 to the Peroxides 6

The chosen reaction conditions differ from those originally employed by the Li group[6] by a higher loading of the oxidant *t*BuOOH (3.0 equiv.) and by the addition of dichloroethane (DCE) as solvent. The former guaranteed full conversion of **1** to the product **6**, which is not necessary in reactions with an added nucleophile that substitutes the peroxide residue and thus regenerates the trapped oxidant. The addition of DCE – in contrast to the "neat" reaction conditions used by Li et al. which only contain decane from the peroxide solution – resulted in cleaner reactions. This

allowed us to conduct them in an NMR tube in deuterated DCE and to follow their progress directly by ^{1}H-NMR without any workup.

One would expect the oxidation of **1** via HAT to *t*BuOO• and subsequent formation of **6** (Scheme 3b) to only show a rather small rate dependency on electronic effects. In contrast, a pathway via single or twofold ET from the nitrogen atom to *t*BuOO• (Scheme 3c) would be expected to show a strong reduction in rate with increasingly electron-withdrawing substituents. We therefore conducted a Hammett plot analysis with amines **1** substituted in the *para*-position of the *N*-aryl ring, by performing competition experiments between different amine couples. This ensures direct access to the relative rates of the reaction between radicals and amines, while the rates of separate experiments for each amine might be controlled by the activation of *t*BuOOH by CuBr only. Separate experiments were also deemed unsuitable in view of the difficulty to ensure equal catalyst concentrations in each experiment, given the very low solubility of CuBr in decane and DCE. Instead of measuring initial rates or conversions at a given time, we monitored the progress of the reaction by in situ ^{1}H-NMR. The relative rates *k* were then calculated from these datasets by the ratio of logarithmic fractional conversions,[14] also called the Ingold-Shaw expression (see the Supporting Information).[15] The Hammett plot of log(*k*) versus σ^+ shows a good linear fit with a slope of $\rho = -0.41$ (Figure 1).

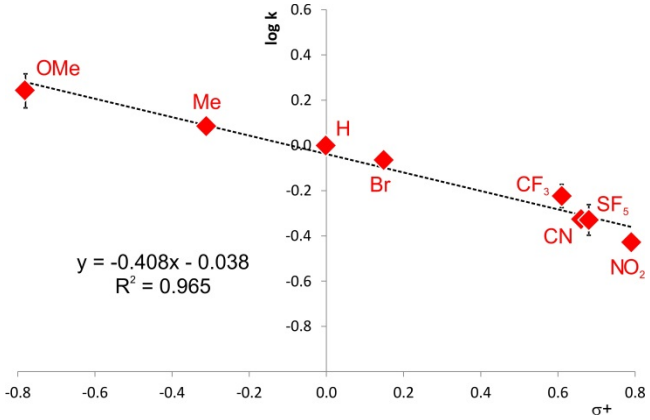

Figure 1. Hammett plot analysis of the formation of substituted peroxides **6**, log *k* refers to relative rate constants from competition experiments.

A similarly good linear fit was obtained when the rate data was plotted against Hammett's σ parameters and against the reduction potential of amines **1a-1h** as determined by cyclic voltammetry, respectively (see the Supporting Information, Figures S2-S3). A correlation with the reduction potential could be regarded as a strong indication for ET being the rate-controlling step;[16] however, HAT processes also have a polar character and the same correlation has been observed in this case as well.[17] For reasons of consistency, a correlation with σ^+ values will be used throughout the manuscript.

While the observed ρ-value is in full agreement with previous measurements of HAT from C-H bonds to *t*BuO•,[18] it is not sufficient to clearly differentiate between ET and HAT. ρ-Values varying between –0.6 and –4.0 (versus σ or σ^+) have been measured for oxidation reactions of amines that were suggested to proceed via ET,[16,19] including the aforementioned study by Ratnikov and Doyle which reported $\rho = -0.76$ as determined from competition experiments with substituted *N,N*-dimethylanilines **2**.[7c,13] Accordingly, we subjected the amines **1a-1h** to a reaction that has been shown to proceed via HAT and not ET, to have a more fitting comparison for the ρ value.

Thus, we carried out a detailed time-resolved kinetic study employing the laser flash photolysis (LFP) technique on the reactions of *N*-aryl THIQs **1** with the cumyloxyl radical ($PhC(CH_3)_2O$•, CumO•), a genuine HAT reagent (Scheme 5).[20]

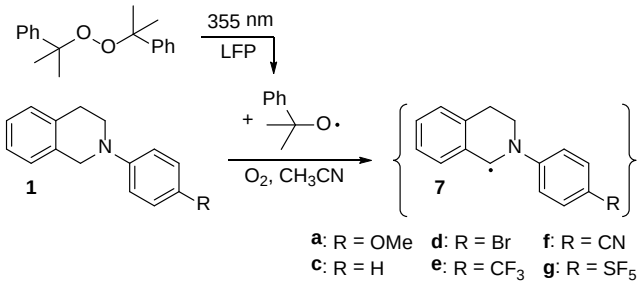

Scheme 5. HAT Reactions from Amines 1a-g to the Cumyloxyl Radical Generated by Laser Flash Photolysis of Dicumyl Peroxide in MeCN

CumO• and *t*BuO• are known to display almost identical HAT reactivities,[21] and both radicals undergo HAT from the α-C–H bonds of tertiary amines with second-order rate constants (k_H) that, in aprotic solvents, exceed 10^8 M^{-1} s^{-1}.[21d,22] While *t*BuO• is characterized by a weak absorption band in the UV region of the spectrum (λ_{max} = 280 nm),[23] CumO• displays an absorption band in the visible region (λ_{max} = 485 nm in aprotic solvents),[24] a feature that makes the direct study of its reactions particularly convenient, employing time-resolved techniques such as LFP. Most importantly, both radicals are relatively weak one-electron oxidants (in MeCN, $E^o_{RO•/RO^-}$ = -0.30 and -0.19 V/SCE, for *t*BuO• and CumO•, respectively), and are known to undergo ET reactions only with substrates characterized by very low oxidation potentials such as polyalkylated ferrocenes.[25]

CumO• was generated by 355 nm LFP of 0.8-1.0 M dicumyl peroxide solutions in MeCN, 2,2,4-trimethylpentane (isooctane), 1,2-dichloroethane (DCE) and 2-methyl-2-butanol (MBOH), respectively. In argon-saturated solution, the strong absorption of carbon radical **7** formed following HAT prevented the determination of the rate constants. As an example, the time-resolved absorption spectra for reaction of CumO• with **1a**, **1c** and **1f** (R = OMe, H and CN, respectively), measured in argon-saturated MeCN solution, are displayed in the Supporting Information (see Figures S57-S59). Accordingly, all the kinetic experiments were carried out in oxygen-saturated solution, where carbon radical **7** is scavenged by fast reaction with O_2.[26]

The second-order rate constants (k_H) for HAT from **1a-1g** to CumO• were obtained from the slope of the observed rate constant (k_{obs}) vs [substrate] plots, the k_{obs} values were measured by following the decay of the CumO• visible absorption band at the different substrate concentrations employed. The strong absorption of **1h** (R = NO2) at the laser excitation wavelength prevented a kinetic study with this substrate.

All the k_{obs} vs [substrate] plots thus obtained are displayed in the Supporting Information (Figures S60-S71). The corresponding k_H values in different solvents are collected in Table 1. Also included in this table are the k_H values measured for reaction of CumO• with **1c-D$_2$**, the derivative of **1c** bearing two deuterium atoms in the benzylic α-position of the amine, and those measured previously for reaction of CumO• with *t*BuOOH in different solvents.[11b]

TABLE 1. Second-Order Rate Constants (k_H) for HAT from *N*-Aryl THIQs 1[a] and *t*BuOOH[b] to the Cumyloxyl Radical (CumO•) Measured in Different Solvents.

Entry	Substrate	Solvent	k_{HAT} ($M^{-1}s^{-1}$)
1	**1a** (OMe)	CH_3CN	$4.8\pm0.10\cdot10^8$
2	**1c** (H)	isooctane	$5.2\pm0.1\cdot10^8$
3	**1c-D$_2$** (H)	isooctane	$2.19\pm0.04\cdot10^8$
4	**1c** (H)	CH_3CN	$2.80\pm0.02\cdot10^8$
5	**1c-D$_2$** (H)	CH_3CN	$1.57\pm0.02\cdot10^8$
6	**1c** (H)	MBOH[c]	$1.98\pm0.06\cdot10^8$
7	**1c** (H)	DCE	$1.61\pm0.08\cdot10^8$
8	**1d** (Br)	CH_3CN	$2.17\pm0.07\cdot10^8$
9	**1e** (CF_3)	CH_3CN	$2.01\pm0.02\cdot10^8$
10	**1f** (CN)	CH_3CN	$1.53\pm0.02\cdot10^8$
11	**1f** (CN)	DCE	$9.58\pm0.02\cdot10^7$
12	**1g** (SF_5)	CH_3CN	$1.65\pm0.02\cdot10^8$
13[b]	*t*BuOOH	CCl_4	$2.5\cdot10^8$
14[b]	*t*BuOOH	benzene	$1.3\cdot10^8$
15[b]	*t*BuOOH	CH_3CN	$8.7\cdot10^6$
16[b]	*t*BuOOH	*t*BuOH	$6.7\cdot10^6$

[a]This work. Measured in oxygen-saturated solution at T = 25°C by following 355 nm LFP of 0.8-1.0 M dicumyl peroxide solutions. The k_H values were obtained from the slope of the k_{obs} vs [substrate] plots, while the k_{obs} values were measured by following the decay of the CumO• visible absorption band at 490 nm. [b]Ref. 11b. [c]MBOH: 2-methyl-2-butanol.

The data displayed in Table 1 show that in the reactions of CumO• with *N*-aryl THIQs **1a-1g** the k_H values decrease with decreasing electron donating ability of the *N*-aryl substituent, in line with the electrophilic character of the abstracting radical.[27] The Hammett plot for HAT from **1a-1g** to CumO• is displayed in Figure 2.

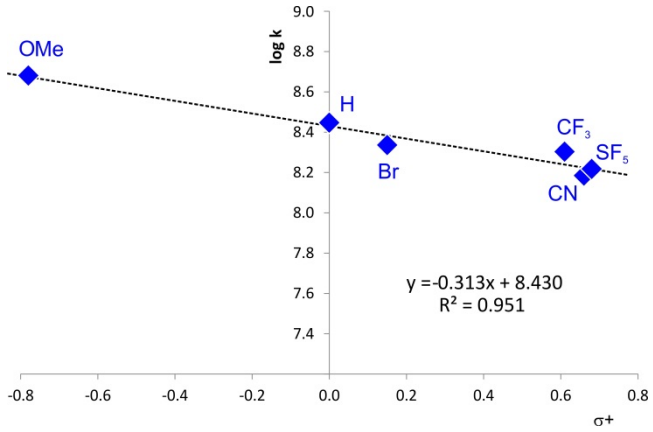

Figure 2. Hammett plot analysis of HAT reactions from amines **1a-g** to the cumyloxyl radical generated by laser flash photolysis in MeCN.

The ρ value for this HAT reaction, –0.31, is clearly similar to the one obtained from the plot displayed in Figure 1, strongly supporting the hypothesis that the key step of these reactions is HAT to an oxyl radical and not ET.

Interestingly, the rate constants for HAT from *N*-aryl THIQs **1a-g** to cumyloxyl measured in acetonitrile were generally higher than the above-mentioned values measured for the corresponding *t*BuOOH (Table 1). The rate constant for HAT from **1c** to CumO•, for example, was determined as $k_H = 2.8\cdot10^8$ $M^{-1}s^{-1}$ in acetonitrile (entry 4), while for HAT from *t*BuOOH a value $k_H = 8.7\cdot10^6$ $M^{-1}s^{-1}$ (entry 15) has been reported.[11b] The solvent effect found for *N*-aryl THIQs **1** was relatively small with the rate constants generally decreasing with increasing solvent polarity (compare entries 2, 4, 6, 7 and 10, 11), in line with previous investigations.[21e,28] In contrast, the solvent effect for HAT from *t*BuOOH has been reported as "dramatic" (entries 13-16).[11b] When the values for the *N*-aryl THIQs are compared with those reported for *t*BuOOH (entries 1-12 vs. 13-16), it is obvious that the amines generally react faster or at least with similar rates. We thus conclude that the common assumption outlined in Scheme 2 that the reactions following catalytic decomposition of *t*BuOOH into radicals are generally driven by peroxyl radicals is not correct. At least in the present case of reactions involving *N*-aryl THIQs **1**, *t*BuO•, which, as mentioned above, exhibits almost the same HAT reactivity as CumO•,[21] will predominantly react by HAT from the amines and not from *t*BuOOH.

For comparison, we computed corresponding Hammett plots at the UM06-2X/6-311+G(2df,2pd)//UM06-2X/6-31+G(d,p) level of DFT (Figure 3). We studied various reaction pathways of the substituted amines **1**, but only address the abstractions with *t*BuO• and *t*BuOO• here.

The best agreement with the experimental Hammett data was achieved with a HAT reaction from amines **1** to *t*BuO•, giving a ρ value of –0.43 against σ^+ (Figure 3a, c.f. Figure 1). In contrast, HAT to *t*BuOO• produced a much higher ρ value of –0.92 against σ^+ (Figure 3b). The greater sensitivity in the hydrogen abstraction with *t*BuOO• is indicative of its later transition state as compared with

*t*BuO•.[16] For comparison, a Hammett plot was constructed using CumO• as the hydrogen abstraction agent for calibration of the method. The resulting sensitivity agreed reasonably well with the experimental value (Figure 3c, c.f. Figure 2).

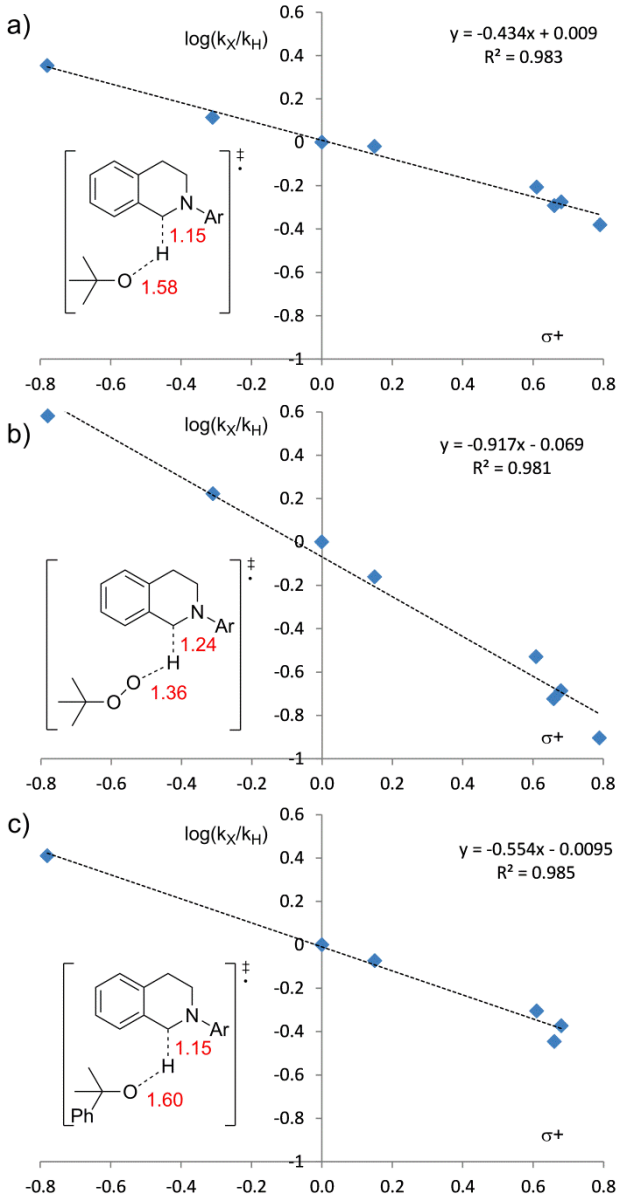

Figure 3. Computational Hammett plot analysis of HAT reactions from amines **1** to the a) *tert*-butoxyl radical, b) *tert*-butylperoxyl radical and c) cumyloxyl radical. Also shown are key distances (Å) in the HAT transition states.

The results obtained from this experimental and computational study (Figures 1-3) provide strong support to the hypothesis that the reaction of Scheme 4 proceeds predominantly by HAT from amines **1** to *t*BuO•, rather than to *t*BuOO•.

For additional experimental information, we also employed the parent amine **1c** in kinetic isotope effect (KIE) experiments, performing separate experiments with **1c** and **1c-D$_2$** (KIE type 1), a competition experiment with **1c** and **1c-D$_2$** (type 2), and an intramolecular competition experiment with **1c-D** (type 3) (Scheme 6). Only the experiment of type 1 can truly reveal whether C-H bond cleavage is involved in the rate-controlling step, while types 2 and 3 might only reflect the relative rates of later steps - information that is nevertheless potentially very useful.[29] As before, we monitored the reaction progress by ^{1}H-NMR and calculated the kinetic isotope effect of the type 2 experiments by the ratio of logarithmic fractional conversions (see the Supporting Information).[14]

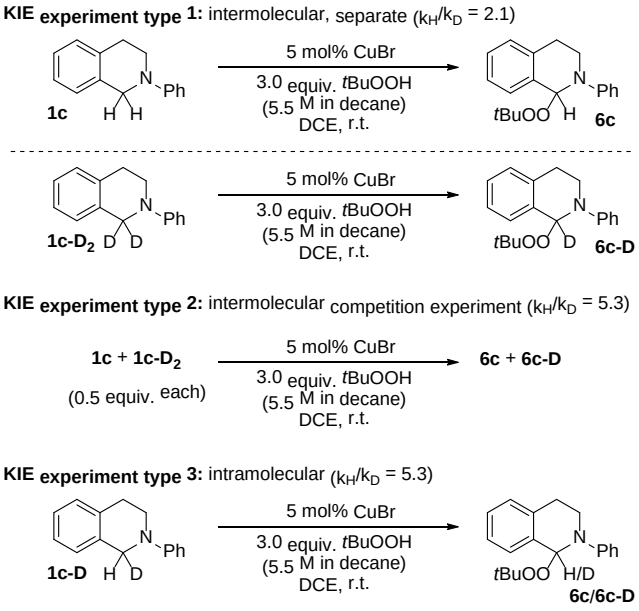

Scheme 6. Kinetic Isotope Effects in the Formation of 6

The values thus obtained were 2.1 ± 0.13, 5.3 ± 0.38 and 5.3 for KIEs of types 1, 2 and 3, respectively. The primary kinetic isotope effect of type 1 clearly indicates that C-H bond cleavage is involved in the rate-controlling step.

Ratnikov and Doyle had measured KIEs of type 2 and 3 for *N*,*N*-dimethylaniline and obtained values of 1.71 and 2.46, respectively.[7c] These significantly smaller values indicate that C-H bond cleavage has a stronger influence on the rate in our system than in Doyle's, supporting HAT and ET as rate controlling steps, respectively. In a previous study with **1c**, using $CuCl_2$ and oxygen as terminal oxidant, we had determined a value of 1.3 for a type 1 experiment, suggesting a secondary KIE due to ET to Cu(II).[30] This lower value, compared with the one obtained here, also supports the suggested mechanisms.

Determining the KIE of type 1 in the laser-flash-photolysis-initiated reaction of Scheme 5 between **1c** and the cumyloxyl-radical gave values of 1.78 and 2.37 in acetonitrile and isooctane, respectively (Table 1, entries 2-5). In additional DFT calculations at the UM06-2X/6-31G+G(d,p) level, we obtained KIE values of 2.7, 2.7 and 4.7 for the reactions between **1** and *t*BuO•, CumO• and *t*BuOO•, respectively. The KIE measured in the type 1 experiment (2.1, Scheme 6) is much closer to the value computed for *t*BuO•

(2.7) than for *t*BuOO• (4.7). The results from these KIE studies support the notion that the formation of **6** proceeds via rate-controlling HAT and involves predominantly *t*BuO•.

In a previous study using Li's original conditions for the oxidative coupling of **1c** with dimethylmalonate, we had found a KIE value of 3.4 for a type 3 experiment.[7b] In Ru-catalyzed reactions of *N*,*N*-dimethylaniline using *t*BuOOH as oxidant, KIE experiments of type 3 had also resulted in lower values of 2.2 and 3.5, respectively.[7a,31]

We thus wondered whether an interconnected system of HAT reactions plays a role, leading to different and relatively high values in type 2 and 3 experiments and making these susceptible to reaction conditions. For *t*BuO•, formed by Cu-catalysis, there is a competition between the HAT reaction with *t*BuOOH (HAT1) and with **1** (HAT2), which is influenced by the individual rate constants k_{HAT1} and k_{HAT2}, respectively, and the concentrations [*t*BuOOH] and [**1c**] (Scheme 7).

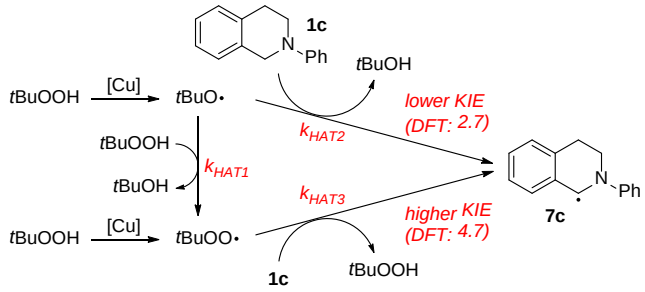

Scheme 7. HAT Sequence Affecting the KIE

As indicated in Scheme 7, our DFT calculations predict a significantly lower KIE for HAT2 than for HAT3, the reaction of *t*BuOO• with **1c**. We thus probed this prediction by changing the reaction conditions in KIE experiments of type 3, in order to vary the relative importance of pathways HAT1 versus HAT2. This would in turn affect the relation of HAT2 versus HAT3 in the formation of radical **7c** as precursor to the observed product **6c** (Table 2).

Table 2. Kinetic Isotope Effect Experiments of Type 3 Using Different Reaction Conditions.[a]

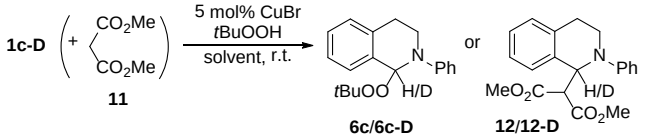

Entry	Equiv. **11**	Equiv. *t*BuOOH	Solvent	Product	KIE[b]
1	0	6.0	DCE	**6c**	8.3
2	0	3.0	DCE	**6c**	5.3
3	0	3.0	CH_3CN	**6c**	4.3
4	1.0	1.0	DCE	**13**	3.0

[a]Using 5.5 M *t*BuOOH in decane. [b]Ratio **6c-D**/**6c** and **12-D**/**12**, respectively, by ^{1}H-NMR.

Using 6.0 equivalents of *t*BuOOH, a very high KIE value of 8.3 was measured (entry 1), compared with the value of 5.3 as determined before under standard conditions (entry 2). Performing the reaction in acetonitrile resulted in a lower KIE with a value of 4.3 (entry 3). Using only one equivalent of *t*BuOOH in the standard reaction was not possible, since the formation of **6** requires the use of two equivalents, one as an oxidant and one as a coupling partner. Therefore, we performed the reaction with one equivalent of *t*BuOOH as oxidant in the presence of one equivalent of dimethylmalonate (**11**) as nucleophile to give product **12**. Under these conditions, a KIE value of 3.0 was determined (entry 4).

These results are in line with the model of Scheme 7. An increased concentration of *t*BuOOH increases the rate of HAT1, thus increasing the relative importance of HAT3 over HAT2 and thereby the overall KIE. In acetonitrile, HAT1 becomes much slower compared with less polar solvents (Table 1, entries 13-14 versus 15), while HAT2 rather increases (Table 1, entry 7 versus 4). Under these conditions, HAT2 will become more favoured than HAT3, resulting in a lower KIE. Finally, by using only one equivalent of *t*BuOOH, HAT1 will be slowed down compared with standard conditions, which again decreases the KIE.

The HAT sequence hypothesized in Scheme 7 was explored with DFT (Figure 4). HAT2 has a computed barrier of 9.6 kcal·mol^{-1}, via transition state **1c-*t*BuO-TS** that is 0.8 kcal·mol^{-1} lower in energy than that for HAT1 in DCE. The preference switches in the gas phase (–1.2 kcal·mol^{-1}). HAT3 has a significantly higher barrier of 19.1 kcal·mol^{-1} via transition state **1c-*t*BuOO-TS**. The general trends drawn from the computed profile are indeed consistent with the KIE data from Table 2 and with the solvent effects seen in Table 1.

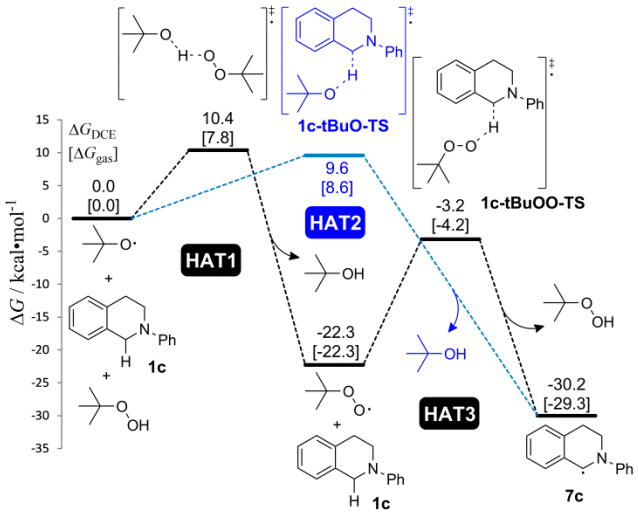

Figure 4. Gibbs free energy profile (kcal/mol) for the competition between *t*BuO• and *t*BuOO•. Values at the stationary points taken from DFT calculations in solution [gas phase]. Black: HAT1 followed by HAT3; blue: HAT2.

The feasibility of an ET mechanism was evaluated by computing the reaction Gibbs free energies in solution for

the electron transfer from **1** to *t*BuO• and *t*BuOO• (Scheme 8). For the solvent used in this reaction, DCE, the computed Gibbs free energies are significantly higher than those for the corresponding HAT processes shown in Figure 4. To explore the limiting case of a very polar solvent, the Gibbs energies were also computed in a high dielectric (H_2O) where the ions are anticipated to be fully solvated and separated. The resulting values remain significantly higher than those for the related HAT processes. The large computed reaction free energies indicate that an ET process with substrate **1** using either *t*BuO• or *t*BuOO• as electron acceptor is unlikely under the reaction conditions.

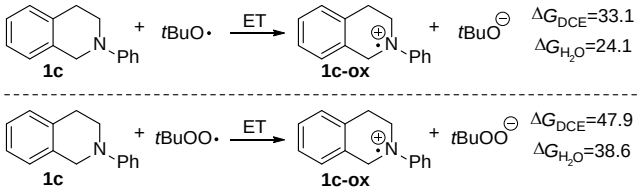

Scheme 8. Computed Reaction Free Energies in Solution for SET at the UM06-2X(CPCM)/6-311+G(2df,2pd)//UM06-2X/6-31+G(d,p) Level

Alternatively, the ET and proton transfer could be proposed as taking place in the same elementary step in a formal proton-coupled electron transfer (PCET) process.[32] If PCET was operative, significant spin density would be expected to accumulate on the nitrogen atom during an electron transfer from the substrate and the transferring hydrogen would exhibit a large partial positive charge.[33] In **1c-tBuO-TS**, the majority of the spin density is localized on the oxygen atom (69%) while only 9% is localized on the nitrogen atom (Figure 5). Furthermore, the NBO partial charge on the transferring hydrogen is only +0.29, which is not much larger than the charge on the axial hydrogen (+0.24) of the other amine methylene group. In comparison, **1c-tBuOO-TS** exhibits a slightly greater spin density on the nitrogen (12%) and a charge on the transferring hydrogen (+0.35) that is still less than expected for a proton transfer.

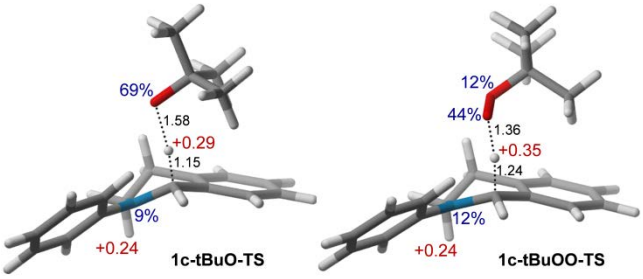

Figure 5. Geometries for transition states **1c-tBuO-TS** and **1c-tBuOO-TS**. Displayed are Mulliken spin densities percentages in blue, NBO partial charges in red, and bond distances (Å) in black.

Taken together, a stepwise ET/proton transfer mechanism is unlikely on account of the prohibitive computed Gibbs energies for the ET (Scheme 8). Alternatively, a PCET mechanism is also unlikely as determined from charge and spin density analysis (Figure 5). Overall, the computed results suggest a direct HAT process.

In light of these results, we wondered about the differences and similarities in the mechanistic proposal put forward by Ratnikov and Doyle. If ET and not HAT is indeed the key step of substrate activation in their system, it must be due to the difference in substrates and reaction conditions – *N,N*-dimethylanilines versus *N*-aryl THIQs, Rh- versus Cu-catalysis, methanol/water versus DCE/decane. This would not be unlikely, as it has been reported that a carotene reacts with *t*BuOO• by ET[34] and that polar protic solvents facilitate ET reactions to peroxyl radicals.[35]

In order to assess this effect, we attempted to study *N,N*-dimethylanilines as substrates and dirhodium caprolactamate as catalyst, respectively, under otherwise identical reaction conditions as shown in Scheme 4. However, the anilines gave too many byproducts, which prevented obtaining a reliable Hammett plot. Substituting CuBr by the rhodium catalyst resulted in rates too high to study the competition between the different amines **1**; even **1h** gave complete conversion after only five minutes. In any case, Ratnikov and Doyle obtained identical KIE's with Cu, Fe, Co, Ru and Rh-catalysts and thus suggested that these activate *t*BuOOH in the same manner without significant involvement in the rest of the reaction.[7c] We did manage to obtain a Hammett plot for the reaction of some *N*-aryl THIQs **1** under the conditions used by Ratnikov and Doyle (Figure 6). Not all of the substituted amines **1** could be used for reasons of solubility and because some of the different products formed could not be distinguished in the ^{1}H-NMR spectra – next to the peroxides **6**, hemiaminal ethers **14** were also formed from methanol.[7c] Although the linear fit is not as good as in the Hammett plots shown above, the trend is very clear.

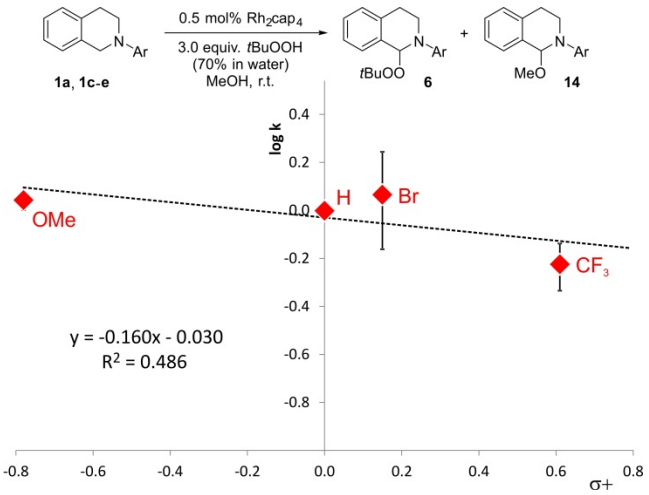

Figure 6. Hammett plot analysis of the oxidation of **1** in MeOH using $Rh_2(cap)_4$ and aqueous *t*BuOOH.

With ρ = –0.16, the slope has become even shallower than before (ρ = –0.41) and is thus consistent with a HAT reaction and not with ET. It differs strongly from the one reported for *N,N*-dimethylanilines under these conditions (ρ = –0.76).[7c,13] The reduced slope could be due to the

strong reduction of k_{HAT1} in polar protic medium (Table 1, entries 13-16), which disfavors involvement of *t*BuOO• in the HAT reaction from **1**.

In order to assess the remaining difference, the structure of the amine substrates, we subjected some *p*-substituted *N*,*N*-dimethylanilines to the time-resolved kinetic study in acetonitrile as shown in Scheme 5 above. The pertinent k_{obs} versus [substrate] plots for reactions with CumO• are displayed in the Supporting Information (Figures S72-S78). The second order rate constants thus obtained were rather similar to those obtained with the *N*-aryl-THIQs and similar kinetic solvent effects were observed for the two series of substrates (see Table S7). The Hammett plot analysis gave a slope of ρ = –0.53 (see Figure S79). The Hammett plots constructed by DFT calculations gave ρ = –0.90 for HAT from the anilines to *t*BuO• and ρ = –1.25 for HAT to *t*BuOO• (see the Supporting Information for details of the kinetic and computational studies). Support for HAT instead of ET was also provided by a previous study of the reaction between *N*,*N*-dimethylanilines and CumOO•.[36] Furthermore, the reduction potentials for **1a**-**h** and similarly substituted anilines lie in the same range (see the Supporting Information and compare with reported values[16a]).

These results suggest the possibility that the reactions studied by Ratnikov and Doyle actually proceed by HAT as well. However, ET cannot be ruled out with certainty.

SUMMARY AND CONCLUSIONS

In summary, the results from the present experimental and computational study clearly indicate that the oxidative coupling of *N*-aryl tetrahydroisoquinolines **1** with *t*BuOOH, catalyzed by CuBr, proceeds via hydrogen atom transfer (HAT) from the amines to directly give an intermediate carbon centered radical **7** (Scheme 9).

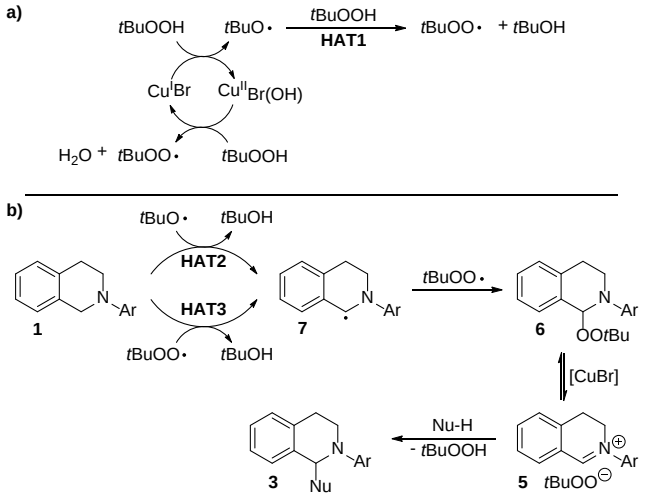

Scheme 9. Mechanistic Proposal for the Oxidative Coupling of Amines 1 with *t*BuOOH

The role of CuBr is to catalyze the decomposition of the oxidant *t*BuOOH into *t*BuO• and *t*BuOO• (Scheme 9a). An additional source of *t*BuOO• is the fast hydrogen atom transfer reaction from *t*BuOOH to *t*BuO• (HAT1). Both *t*BuO• and *t*BuOO• can be hydrogen atom acceptors in reactions with amines **1**, forming radical **7** (HAT2 and HAT3, respectively, Scheme 9b). This reacts further to peroxide **6**, which decomposes to the iminium intermediate **5** by Lewis-acid catalysis, leading to the coupling products **3** after attack from various nucleophiles.

In contrast to what is often proposed in this and related reactions, *t*BuO• was found to be the dominant acceptor radical in the reaction with **1**, in line with the finding that the rate constant of HAT2 is generally larger or at least similar to the rate constant of HAT1. Also, HAT2 is decreased less by solvent polarity than HAT1. Accordingly, the relative contribution of HAT2 and HAT3 to the formation of the amine-peroxide products **6** is susceptible to the exact reaction conditions. This could be qualitatively demonstrated by changes in intramolecular kinetic isotope effects, which ranged from 3 to 8, depending on the concentration of *t*BuOOH or the solvent.

The previous proposal by Ratnikov and Doyle of an electron transfer pathway in the formation of peroxide products from *N*-aryl amines is not supported by this study. Instead, our results indicate that also in the highly polar reaction medium used in their study – a mixture of methanol and water – substrate **1** is activated by HAT. However, a different mechanism in their reaction of study cannot be ruled out as they used a different catalyst and different amines (*N*,*N*-dimethylanilines).

The experimental results obtained in this study cannot clearly explain the formation of the observed product **6** from the putative radical **7** (Scheme 9b). However, the previously suggested[7b] radical combination appears reasonable. In a first instance, the copper-catalyzed decomposition of *t*BuOOH produces *t*BuO• and *t*BuOO• at the same rate. The majority of *t*BuO• reacts via HAT2, forming the majority of C-radical **7**, thus leading to a relatively high concentration of unreacted *t*BuOO•. It has been reported that dimerization or other self-decomposition pathways of tertiary peroxyl radicals are slow while their reaction with carbon radicals is fast.[37] Accordingly, it appears reasonable that under these conditions, the amino-peroxides **6** are formed by radical combination in high yields. It has also been suggested[8c] that such reactions with *t*BuOO• fulfill the criteria of the persistent radical effect.[38] Nevertheless, these are reactive species and our attempts to observe them in the present reaction by EPR spectroscopy have been in vain. Whether the bond-forming event that produces peroxide **6** is preceded by ET, as suggested before,[7c] remains questionable – at least in the nonpolar medium employed here which would disfavor the creation of charge-separated species.

The presence of nucleophiles, required to synthesize coupling products **3** and usually present in all synthetic studies, should in principle not affect the mechanisms discussed in the present study. Studies monitoring the reaction progress indicate this to be the case for various nucleophiles.[7b] Nucleophiles that can be involved in fast HAT

reactions would result in diminished yields and byproducts. The reported reaction between **1c** and 2-naphthol, which led to the formation of significant amounts of binaphthol, could be such a case.[6f]

Apart from clarifying mechanistic details of a reaction that inspired researchers world-wide, the present study also illustrates some issues that could be relevant for all other oxidative coupling reactions utilizing a similar combination of redox-active catalyst and *t*BuOOH.[39] The common assumption that oxidative coupling reactions with *t*BuOOH are predominantly driven by *t*BuOO• should be treated with caution. While its formation by HAT from *t*BuOOH to *t*BuO• is fast, HAT reactions from the substrates employed can be faster. Also, the interplay of HAT reactions 1, 2 and 3 can significantly alter the results of kinetic isotope studies, an effect that should be considered when comparing results obtained under different conditions.

ASSOCIATED CONTENT

Supporting Information. Experimental and computational details including product characterization and kinetic experiments. This material is available free of charge via the Internet at http://pubs.acs.org.

AUTHOR INFORMATION

Corresponding Authors

bietti@uniroma2.it
thiel@mpi-muelheim.mpg.de
klusi@mpi-muelheim.mpg.de

Present Addresses

§ Present address: Department of Chemistry, Indian Institute of Technology Bombay, Powai, Mumbai 400076, India

ACKNOWLEDGMENT

Financial support from the DFG (Heisenberg scholarship to M.K., KL 2221/4-1) and the MPI für Kohlenforschung is gratefully acknowledged. E.B. and M.K. thank the NMR department for their generous support and Christian Wille and Nobuhito Uemiya for CV measurements. M.S. and M.B. gratefully acknowledge financial support from the Ministero dell'Istruzione dell'Università e della Ricerca (MIUR), project 2010PFLRJR (PRIN 2010-2011), and thank Prof. Lorenzo Stella for the use of a LFP equipment. The authors thank M. O. Ratnikov and M. P. Doyle for kindly sharing their data.

REFERENCES

(1) a) Girard, S. A.; Knauber, T.; Li, C.-J. *Angew. Chem. Int. Ed.* **2014**, *53*, 74-100; b) Zheng, C.; You, S.-L. *RSC Adv.* **2014**, *4*, 6173-6214; c) Gulzar, N.; Schweitzer-Chaput, B.; Klussmann, M. *Catal. Sci. Technol.* **2014**, *4*, 2778-2796; d) Liu, C.; Zhang, H.; Shi, W.; Lei, A. *Chem. Rev.* **2011**, *111*, 1780-1824; e) Yeung, C. S.; Dong, V. M. *Chem. Rev.* **2011**, *111*, 1215-1292.

(2) a) Mitchell, E. A.; Peschiulli, A.; Lefevre, N.; Meerpoel, L.; Maes, B. U. W. *Chem. Eur. J.* **2012**, *18*, 10092-10142; b) Jones, K. M.; Klussmann, M. *Synlett* **2012**, *23*, 159-162; c) Qin, Y.; Lv, J.; Luo, S. *Tetrahedron Lett.* **2014**, *55*, 551-558.

(3) a) Murata, S.; Miura, M.; Nomura, M. *Chem. Commun.* **1989**, 116-118; b) Murata, S.; Teramoto, K.; Miura, M.; Nomura, M. *Bull. Chem. Soc. Jpn.* **1993**, *66*, 1297-1298; c) Murahashi, S.-I.; Komiya, N.; Terai, H.; Nakae, T. *J. Am. Chem. Soc.* **2003**, *125*, 15312-15313.

(4) For examples using TBHP as oxidant, see: a) Catino, A. J.; Nichols, J. M.; Nettles, B. J.; Doyle, M. P. *J. Am. Chem. Soc.* **2006**, *128*, 5648-5649; b) Sud, A.; Sureshkumar, D.; Klussmann, M. *Chem. Commun.* **2009**, 3169-3171; c) Han, W.; Ofial, A. R. *Chem. Commun.* **2009**, 5024-5026; d) Kumar, R. A.; Saidulu, G.; Prasad, K. R.; Kumar, G. S.; Sridhar, B.; Reddy, K. R. *Adv. Synth. Catal.* **2012**, *354*, 2985-2991; e) Zhang, Y.; Luo, S.; Feng, B.; Zhu, C. *Chin. J. Chem.* **2012**, *30*, 2741-2746.

(5) For examples using other oxidants, see: a) Tsang, A. S.-K.; Todd, M. H. *Tetrahedron Lett.* **2009**, *50*, 1199-1202; b) Chu, L.; Qing, F.-L. *Chem. Commun.* **2010**, *46*, 6285-6287; c) Singhal, S.; Jain, S. L.; Sain, B. *Adv. Synth. Catal.* **2010**, *352*, 1338-1344; d) Richter, H.; García Mancheño, O. *Eur. J. Org. Chem.* **2010**, 4460-4467; e) Shu, X.-Z.; Yang, Y.-F.; Xia, X.-F.; Ji, K.-G.; Liu, X.-Y.; Liang, Y.-M. *Org. Biomol. Chem.* **2010**, *8*, 4077-4079; f) Condie, A. G.; González-Gómez, J. C.; Stephenson, C. R. J. *J. Am. Chem. Soc.* **2010**, *132*, 1464-1465; g) Alagiri, K.; Devadig, P.; Prabhu, K. R. *Chem. Eur. J.* **2012**, *18*, 5160-5164; h) Perepichka, I.; Kundu, S.; Hearne, Z.; Li, C.-J. *Org. Biomol. Chem.* **2015**, 447-451; i) Tanoue, A.; Yoo, W.-J.; Kobayashi, S. *Org. Lett.* **2014**, *16*, 2346-2349.

(6) a) Li, Z.; Li, C.-J. *J. Am. Chem. Soc.* **2004**, *126*, 11810-11811; b) Li, Z.; Li, C.-J. *Org. Lett.* **2004**, *6*, 4997-4999; c) Li, Z.; Li, C.-J. *J. Am. Chem. Soc.* **2005**, *127*, 3672-3673; d) Li, Z.; Li, C.-J. *J. Am. Chem. Soc.* **2005**, *127*, 6968-6969; e) Li, Z.; Li, C.-J. *Eur. J. Org. Chem.* **2005**, 3173-3176; f) Li, Z.; Bohle, D. S.; Li, C.-J. *Proc. Natl. Acad. Sci. U.S.A.* **2006**, *103*, 8928-8933.

(7) a) Wang, M.-Z.; Zhou, C.-Y.; Wong, M.-K.; Che, C.-M. *Chem. Eur. J.* **2010**, *16*, 5723-5735; b) Boess, E.; Schmitz, C.; Klussmann, M. *J. Am. Chem. Soc.* **2012**, *134*, 5317-5325; c) Ratnikov, M. O.; Doyle, M. P. *J. Am. Chem. Soc.* **2013**, *135*, 1549-1557; d) Cheng, G.-J.; Song, L.-J.; Yang, Y.-F.; Zhang, X.; Wiest, O.; Wu, Y.-D. *ChemPlusChem* **2013**, *78*, 943-951; e) Zhang, C.; Liu, C.; Shao, Y.; Bao, X.; Wan, X. *Chem. Eur. J.* **2013**, *19*, 17917-17925; f) Tsang, A. S. K.; Park, S. J.; Todd, M. H. *Mechanisms of Cross-Dehydrogenative-Coupling Reactions* in *From C-H to C-C Bonds: Cross-Dehydrogenative-Coupling*; Li, C.-J., Ed.; The Royal Society of Chemistry: 2015, p 254-294.

(8) a) Kharasch, M. S.; Fono, A. *J. Org. Chem.* **1959**, *24*, 72-78; b) Minisci, F.; Fontana, F.; Araneo, S.; Recupero, F.; Banfi, S.; Quici, S. *J. Am. Chem. Soc.* **1995**, *117*, 226-232; c) Bravo, A.; Bjørsvik, H.-R.; Fontana, F.; Liguori, L.; Minisci, F. *J. Org. Chem.* **1997**, *62*, 3849-3857; d) McLaughlin, E. C.; Choi, H.; Wang, K.; Chiou, G.; Doyle, M. P. *J. Org. Chem.* **2009**, *74*, 730-738; e) Shi, E.; Shao, Y.; Chen, S.; Hu, H.; Liu, Z.; Zhang, J.; Wan, X. *Org. Lett.* **2012**, *14*, 3384-3387; f) Tan, B.; Toda, N.; Barbas, C. F. *Angew. Chem. Int. Ed.* **2012**, *51*, 12538-12541; g) Yu, H.; Shen, J. *Org. Lett.* **2014**, *16*, 3204-3207.

(9) a) Kharasch, M. S.; Fono, A.; Nudenberg, W.; Bischof, B. *J. Org. Chem.* **1952**, *17*, 207-220; b) Kochi, J. K. *Tetrahedron* **1962**, *18*, 483-497.

(10) Sometimes erroneously called the Haber-Weiss cycle, see: Koppenol, W. H. *Redox Report* **2001**, *6*, 229-234.

(11) a) Paul, H.; Small, R. D.; Scaiano, J. C. *J. Am. Chem. Soc.* **1978**, *100*, 4520-4527; b) Avila, D. V.; Ingold, K. U.; Lusztyk, J.; Green, W. H.; Procopio, D. R. *J. Am. Chem. Soc.* **1995**, *117*, 2929-2930.

(12) a) Tsang, A. S.-K.; Jensen, P.; Hook, J. M.; Hashmi, A. S. K.; Todd, M. H. *Pure Appl. Chem.* **2011**, *83*, 655-665; b) Boess, E.; Sureshkumar, D.; Sud, A.; Wirtz, C.; Farès, C.; Klussmann, M. *J. Am. Chem. Soc.* **2011**, *133*, 8106-8109.

(13) In the original report, a steeper slope was reported, due to an error of calculation. Re-evaluation of the data gave $\rho = -1.1$

against σ and ρ = –0.76 against σ^+ (with a worse linear correlation). M. O. Ratnikov, M. P. Doyle, personal communication.

(14) a) Ingold, C. K.; Shaw, F. R. *J. Chem. Soc.* **1927**, 2918-2926; b) Melander, L.; William H. Saunders, J. *Reaction Rates of Isotopic Molecules*; John Wiley & Sons, 1980.

(15) Brown, H. C.; Wang, K. K.; Scouten, C. G. *Proc. Natl. Acad. Sci. U.S.A.* **1980**, *77*, 698-702.

(16) a) Goto, Y.; Watanabe, Y.; Fukuzumi, S.; Jones, J. P.; Dinnocenzo, J. P. *J. Am. Chem. Soc.* **1998**, *120*, 10762-10763; b) Baciocchi, E.; Lanzalunga, O.; Lapi, A.; Manduchi, L. *J. Am. Chem. Soc.* **1998**, *120*, 5783-5787; c) Baciocchi, E.; Bietti, M.; Gerini, M. F.; Lanzalunga, O. *J. Org. Chem.* **2005**, *70*, 5144-5149.

(17) Wang, Y.; Kumar, D.; Yang, C.; Han, K.; Shaik, S. *J. Phys. Chem. B* **2007**, *111*, 7700-7710.

(18) a) Uneyama, K.; Namba, H.; Oae, S. *Bull. Chem. Soc. Jpn.* **1968**, *41*, 1928-1937; b) Zavitsas, A. A.; Pinto, J. A. *J. Am. Chem. Soc.* **1972**, *94*, 7390-7396; c) Jones, M. J.; Moad, G.; Rizzardo, E.; Solomon, D. H. *J. Org. Chem.* **1989**, *54*, 1607-1611; d) Kim, S. S.; Kim, S. Y.; Ryou, S. S.; Lee, C. S.; Yoo, K. H. *J. Org. Chem.* **1993**, *58*, 192196.

(19) a) Burka, L. T.; Guengerich, F. P.; Willard, R. J.; Macdonald, T. L. *J. Am. Chem. Soc.* **1985**, *107*, 2549-2551; b) Shearer, J.; Zhang, C. X.; Hatcher, L. Q.; Karlin, K. D. *J. Am. Chem. Soc.* **2003**, *125*, 12670-12671.

(20) Salamone, M.; Bietti, M. *Acc. Chem. Res.* **2015**, *48*, 2895-2903.

(21) a) Baignee, A.; Howard, J. A.; Scaiano, J. C.; Stewart, L. C. *J. Am. Chem. Soc.* **1983**, *105*, 6120-6123; b) Valgimigli, L.; Banks, J. T.; Ingold, K. U.; Lusztyk, J. *J. Am. Chem. Soc.* **1995**, *117*, 9966-9971; c) Sheeller, B.; Ingold, K. U. *J. Chem. Soc., Perkin Trans. 2* **2001**, 480-486; d) Pischel, U.; Nau, W. M. *J. Am. Chem. Soc.* **2001**, *123*, 9727-9737; e) Salamone, M.; Bietti, M. *Synlett* **2014**, *25*, 1803-1816.

(22) a) Griller, D.; Howard, J. A.; Marriott, P. R.; Scaiano, J. C. *J. Am. Chem. Soc.* **1981**, *103*, 619-623; b) Finn, M.; Friedline, R.; Suleman, N. K.; Wohl, C. J.; Tanko, J. M. *J. Am. Chem. Soc.* **2004**, *126*, 7578-7584; c) Salamone, M.; DiLabio, G. A.; Bietti, M. *J. Am. Chem. Soc.* **2011**, *133*, 16625-16634.

(23) Tsentalovich, Y. P.; Kulik, L. V.; Gritsan, N. P.; Yurkovskaya, A. V. *J. Phys. Chem. A* **1998**, *102*, 7975-7980.

(24) a) Baciocchi, E.; Bietti, M.; Salamone, M.; Steenken, S. *J. Org. Chem.* **2002**, *67*, 2266-2270; b) Avila, D. V.; Ingold, K. U.; Di Nardo, A. A.; Zerbetto, F.; Zgierski, M. Z.; Lusztyk, J. *J. Am. Chem. Soc.* **1995**, *117*, 2711-2718.

(25) a) Bietti, M.; DiLabio, G. A.; Lanzalunga, O.; Salamone, M. *J. Org. Chem.* **2010**, *75*, 5875-5881; b) Bietti, M.; DiLabio, G. A.; Lanzalunga, O.; Salamone, M. *J. Org. Chem.* **2011**, *76*, 1789-1794.

(26) Maillard, B.; Ingold, K. U.; Scaiano, J. C. *J. Am. Chem. Soc.* **1983**, *105*, 5095-5099.

(27) Roberts, B. P. *Chem. Soc. Rev.* **1999**, *28*, 25-35.

(28) Bietti, M.; Salamone, M. *Org. Lett.* **2010**, *12*, 3654-3657.

(29) Simmons, E. M.; Hartwig, J. F. *Angew. Chem. Int. Ed.* **2012**, *51*, 3066-3072.

(30) Scott, M.; Sud, A.; Boess, E.; Klussmann, M. *J. Org. Chem.* **2014**, *79*, 12033-12040.

(31) Murahashi, S.-I.; Naota, T.; Yonemura, K. *J. Am. Chem. Soc.* **1988**, *110*, 8256-8528.

(32) Weinberg, D. R.; Gagliardi, C. J.; Hull, J. F.; Murphy, C. F.; Kent, C. A.; Westlake, B. C.; Paul, A.; Ess, D. H.; McCafferty, D. G.; Meyer, T. J. *Chem. Rev.* **2012**, *112*, 4016-4093.

(33) Sirjoosingh, A.; Hammes-Schiffer, S. *J. Phys. Chem. A* **2011**, *115*, 2367-2377.

(34) Jomová, K.; Kysel, O.; Madden, J. C.; Morris, H.; Enoch, S. J.; Budzak, S.; Young, A. J.; Cronin, M. T. D.; Mazur, M.; Valko, M. *Chem. Phys. Lett.* **2009**, *478*, 266-270.

(35) Jovanovic, S. V.; Jankovic, I.; Josimovic, L. *J. Am. Chem. Soc.* **1992**, *114*, 9018-9021.

(36) Fukuzumi, S.; Shimoosako, K.; Suenobu, T.; Watanabe, Y. *J. Am. Chem. Soc.* **2003**, *125*, 9074-9082.

(37) Ingold, K. U. *Acc. Chem. Res.* **1969**, *2*, 1-9.

(38) Studer, A. *Chem. Soc. Rev.* **2004**, *033*, 267-273.

(39) For example, see: a) Murahashi, S.-I.; Naota, T.; Kuwabara, T.; Saito, T.; Kumobayashi, H.; Akutagawa, S. *J. Am. Chem. Soc.* **1990**, *112*, 7820-7822; b) Kirner, H.-J.; Schwarzenbach, F.; van der Schaaf, P. A.; Hafner, A.; Rast, V.; Frey, M.; Nesvadba, P.; Rist, G. *Adv. Synth. Catal.* **2004**, *346*, 554-560; c) Li, Z.; Li, C.-J. *J. Am. Chem. Soc.* **2006**, *128*, 56-57; d) Pan, S.; Liu, J.; Li, H.; Wang, Z.; Guo, X.; Li, Z. *Org. Lett.* **2010**, *12*, 1932-1935; e) Hu, Y. L.; Jiang, H.; Lu, M. *Green Chem.* **2011**, *13*, 3079-3087; f) Ghobrial, M.; Schnürch, M.; Mihovilovic, M. D. *J. Org. Chem.* **2011**, *76*, 8781-8793; g) Chen, L.; Shi, E.; Liu, Z.; Chen, S.; Wei, W.; Li, H.; Xu, K.; Wan, X. *Chem. Eur. J.* **2011**, *17*, 4085-4089; h) Wagner, A.; Hampel, N.; Zipse, H.; Ofial, A. R. *Org. Lett.* **2015**, *17*, 4770-4773; i) Yadav, A. K.; Yadav, L. D. S. *Synlett* **2015**, *26*, 1026-1030.

Graphic entry for the Table of Contents (TOC):

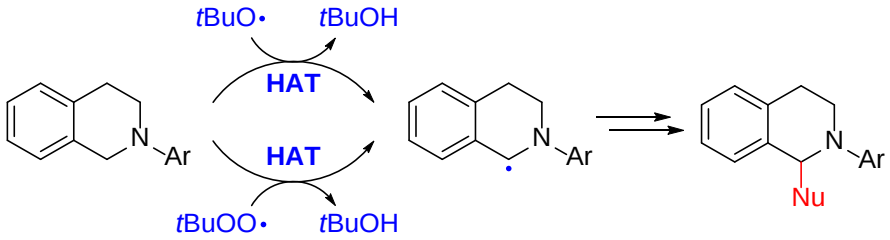

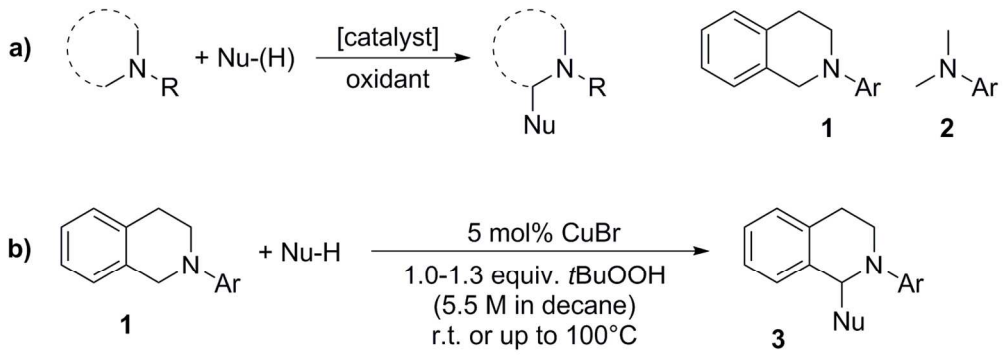

Scheme 1
135x48mm (300 x 300 DPI)

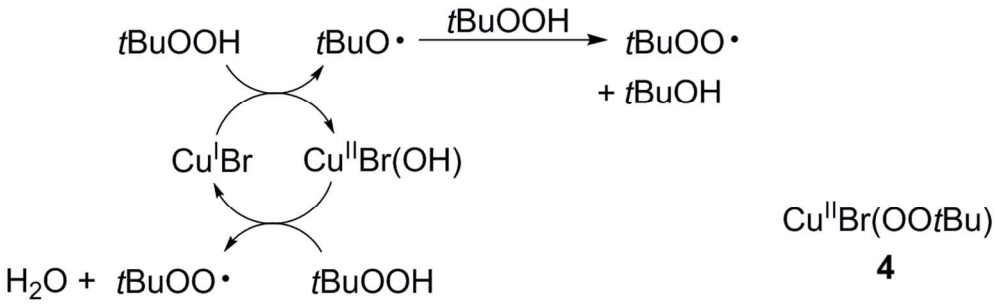

Scheme 2
107x34mm (300 x 300 DPI)

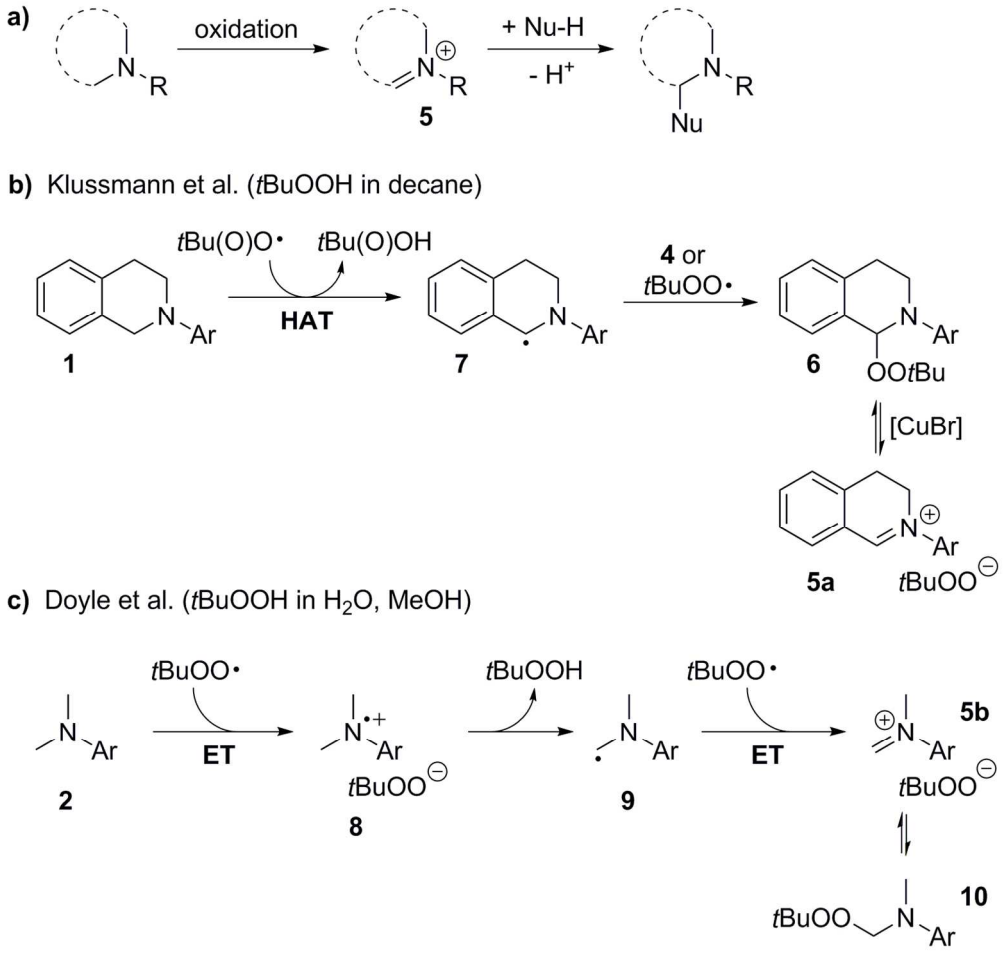

Scheme 3
136x129mm (300 x 300 DPI)

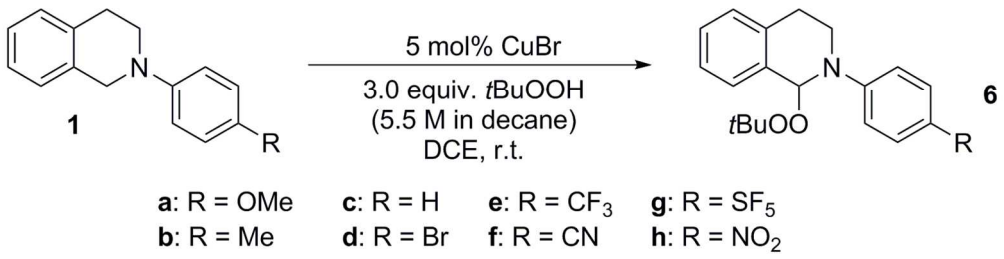

a: R = OMe **c**: R = H **e**: R = CF_3 **g**: R = SF_5
b: R = Me **d**: R = Br **f**: R = CN **h**: R = NO_2

Scheme 4
133x34mm (300 x 300 DPI)

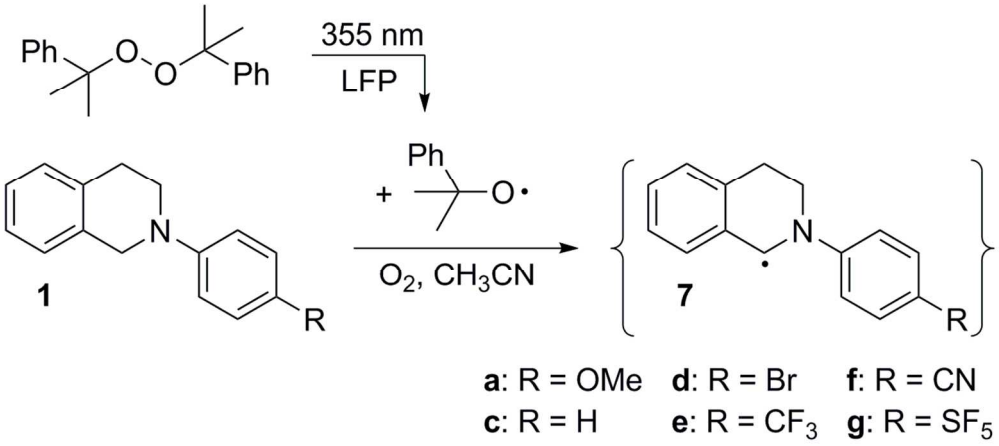

Scheme 5
114x51mm (300 x 300 DPI)

KIE experiment type 1: intermolecular, separate (k_H/k_D = 2.1)

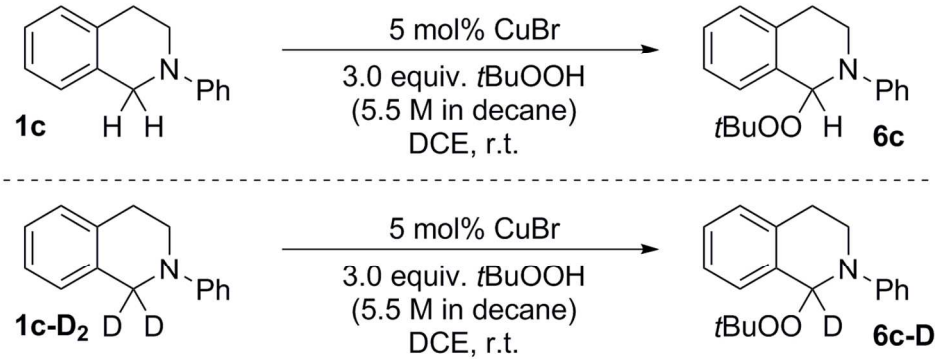

KIE experiment type 2: intermolecular competition experiment (k_H/k_D = 5.3)

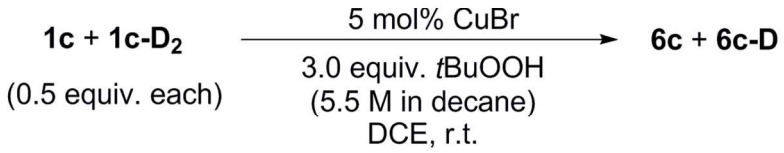

KIE experiment type 3: intramolecular (k_H/k_D = 5.3)

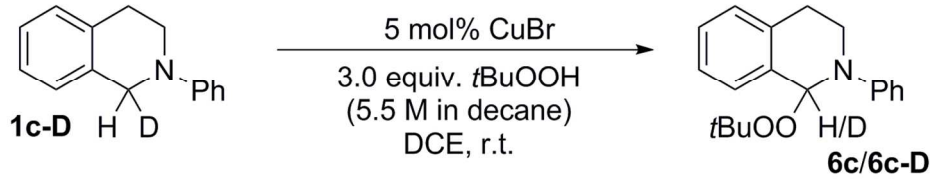

Scheme 6
121x116mm (300 x 300 DPI)

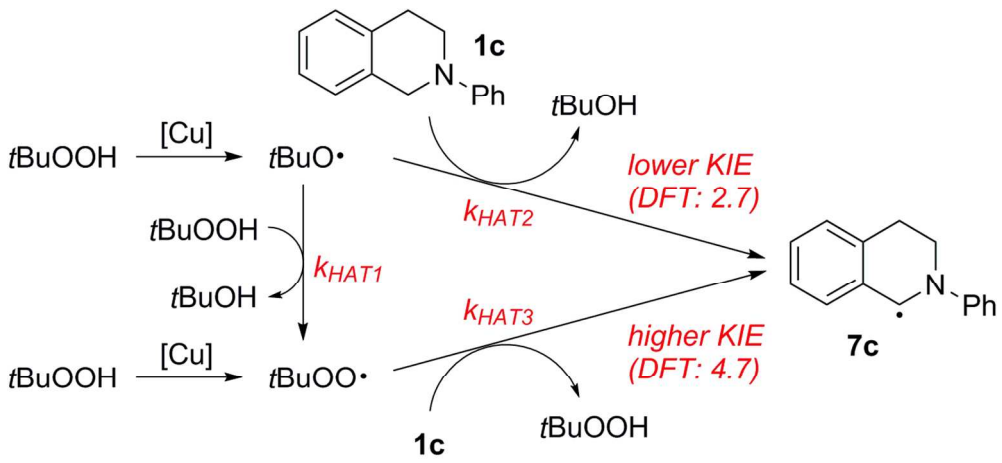

Scheme 7
121x56mm (300 x 300 DPI)

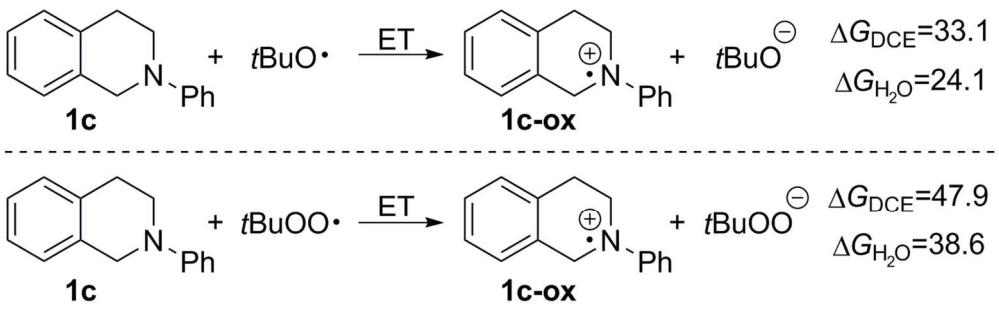

Scheme 8
120x37mm (300 x 300 DPI)

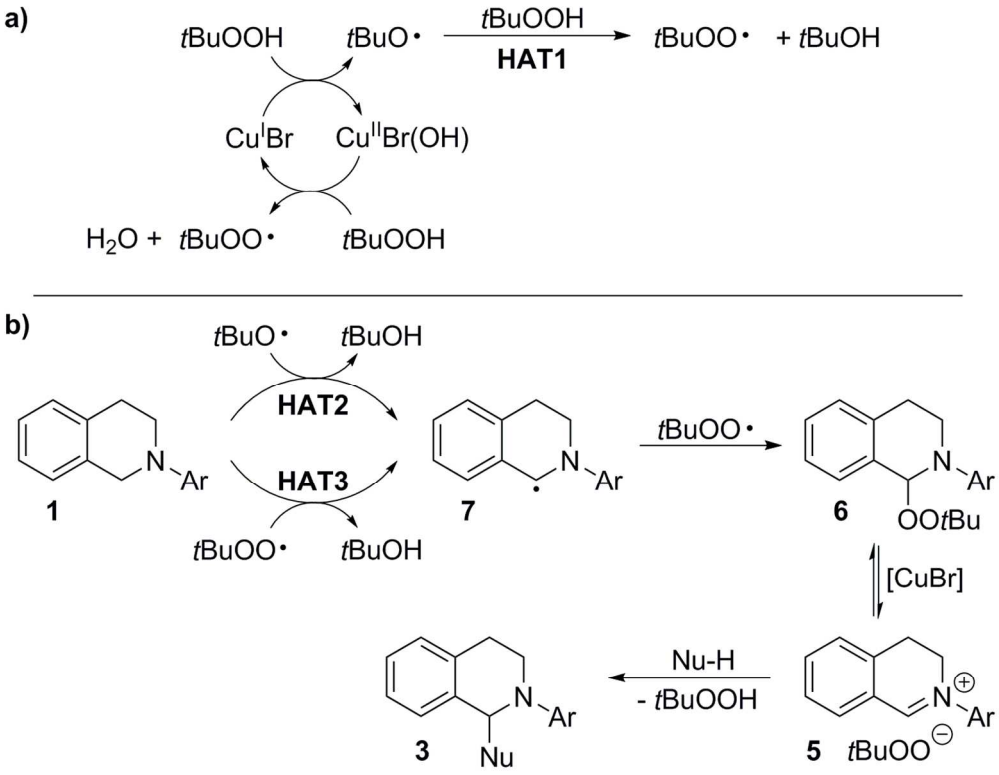

Scheme 9
128x99mm (300 x 300 DPI)

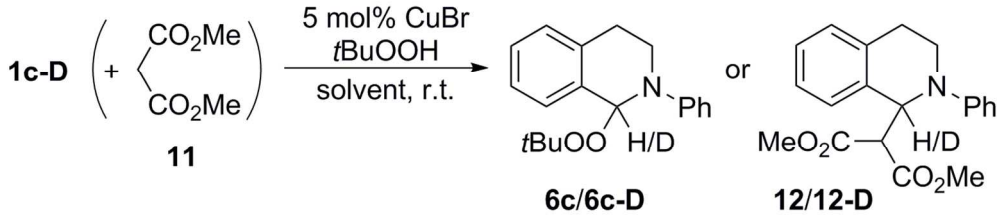

Table 2
124x28mm (300 x 300 DPI)

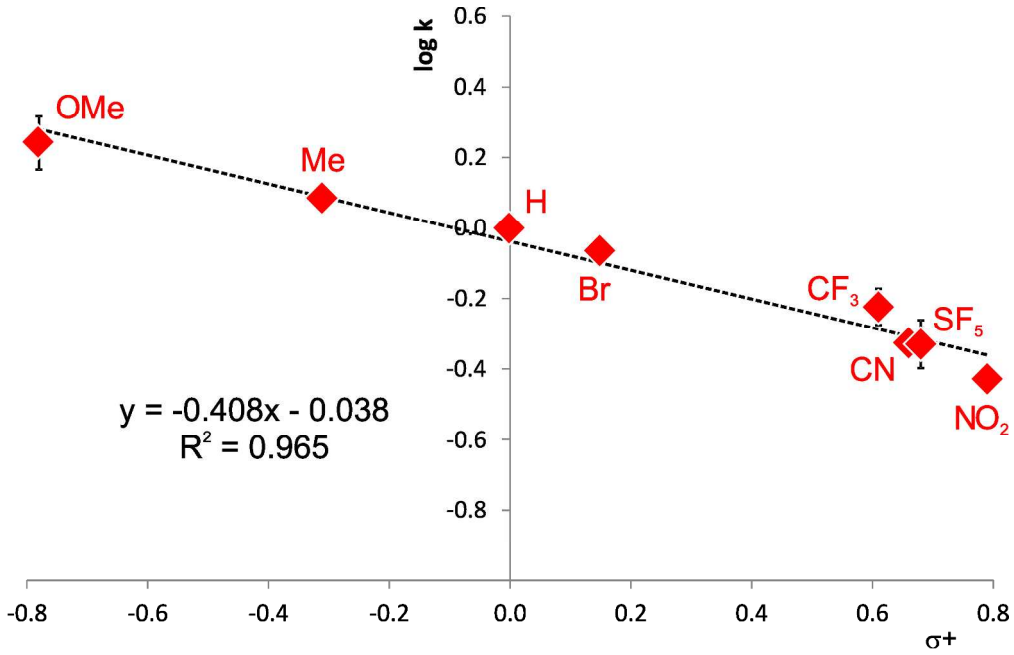

Figure 1
262x168mm (300 x 300 DPI)

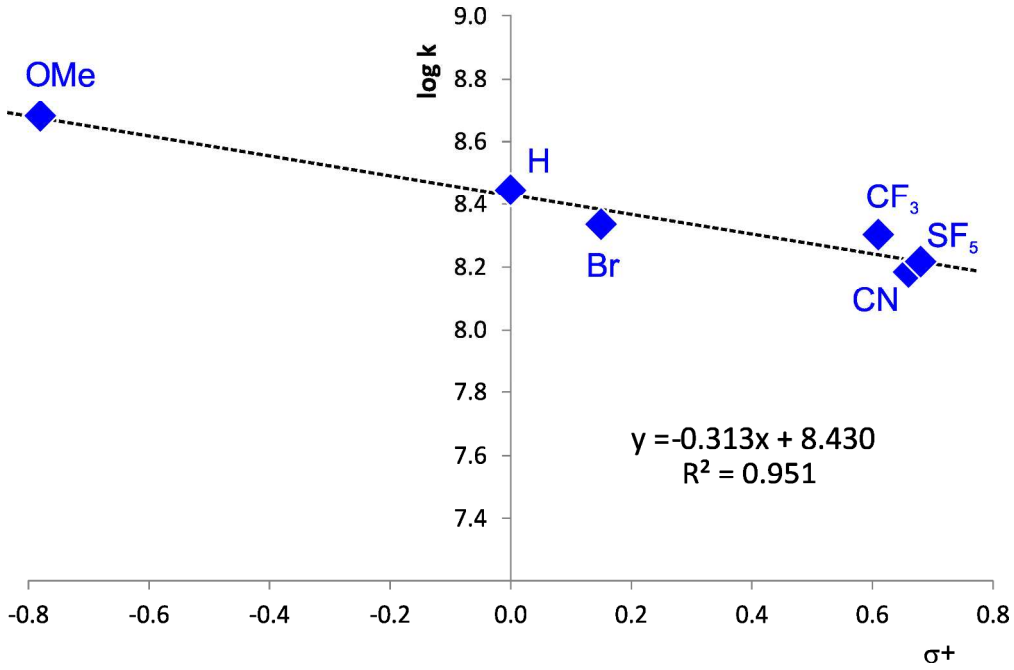

Figure 2
258x169mm (300 x 300 DPI)

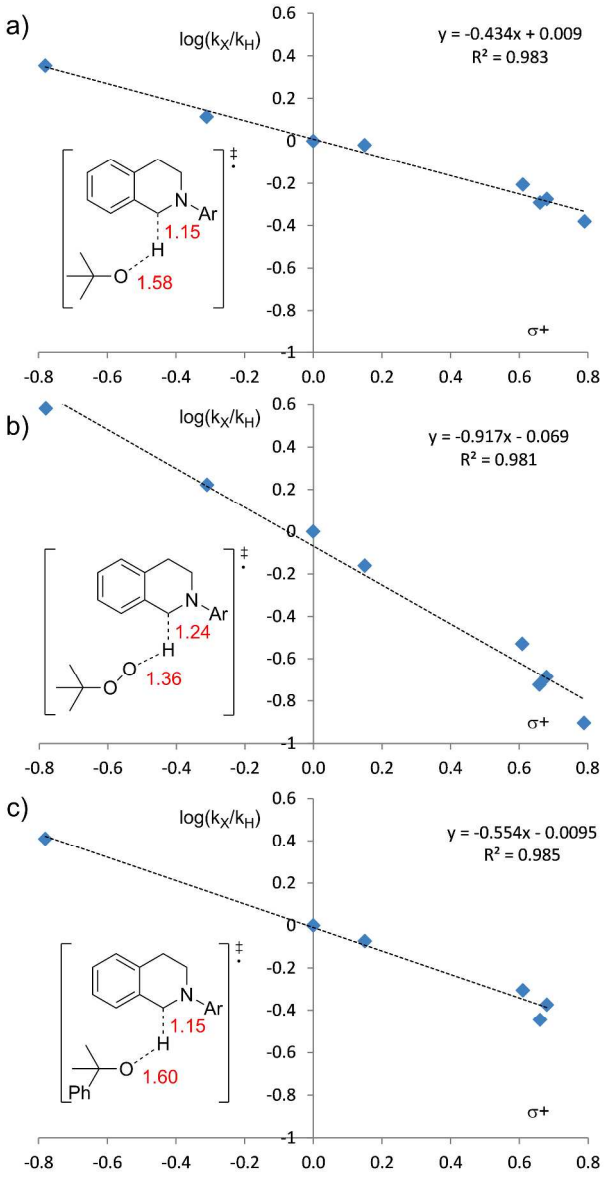

Figure 3
224x430mm (600 x 600 DPI)

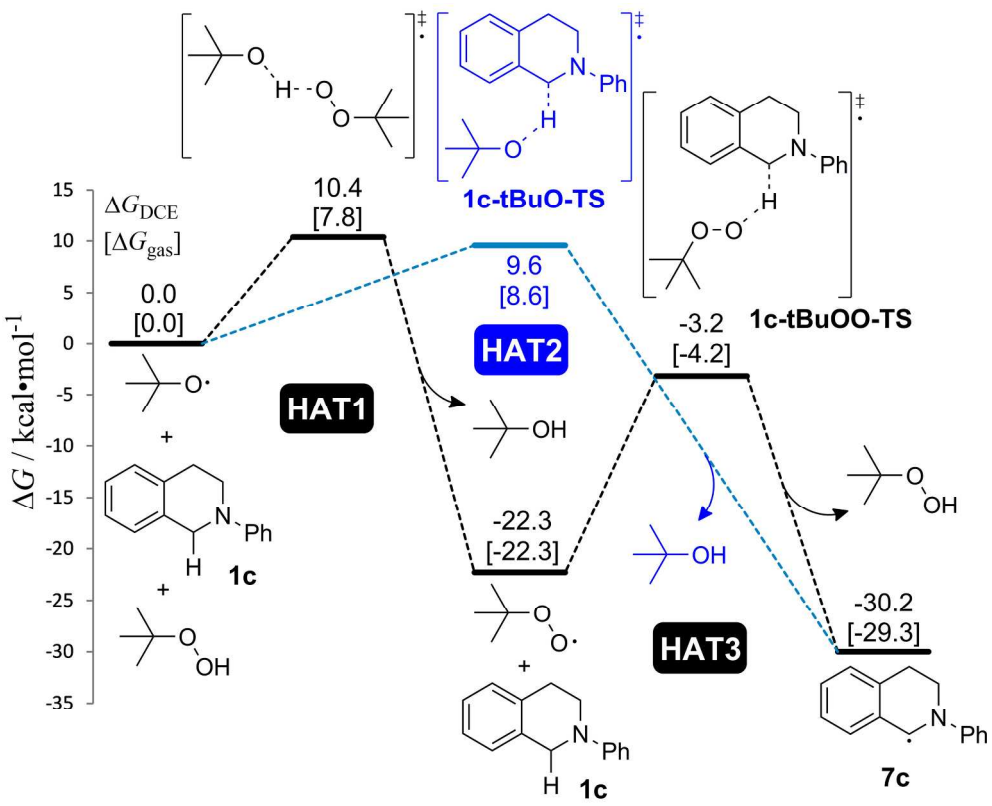

Figure 4
108x87mm (600 x 600 DPI)

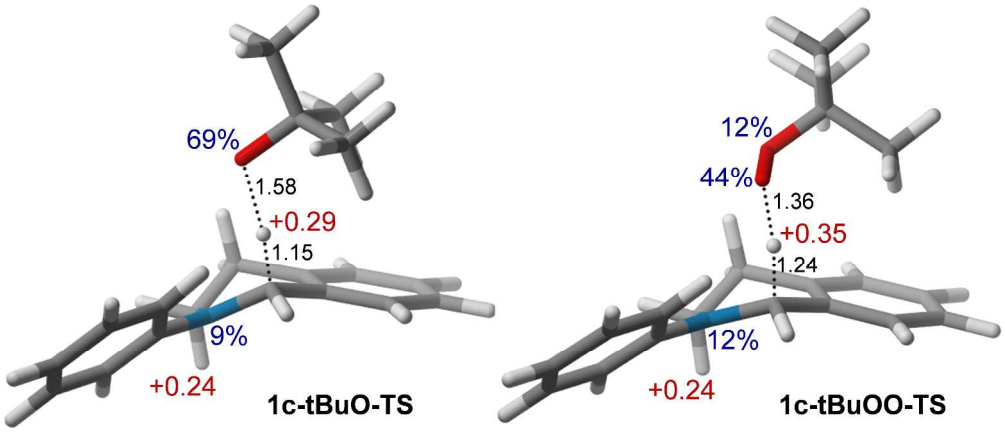

Figure 5
1811x786mm (96 x 96 DPI)

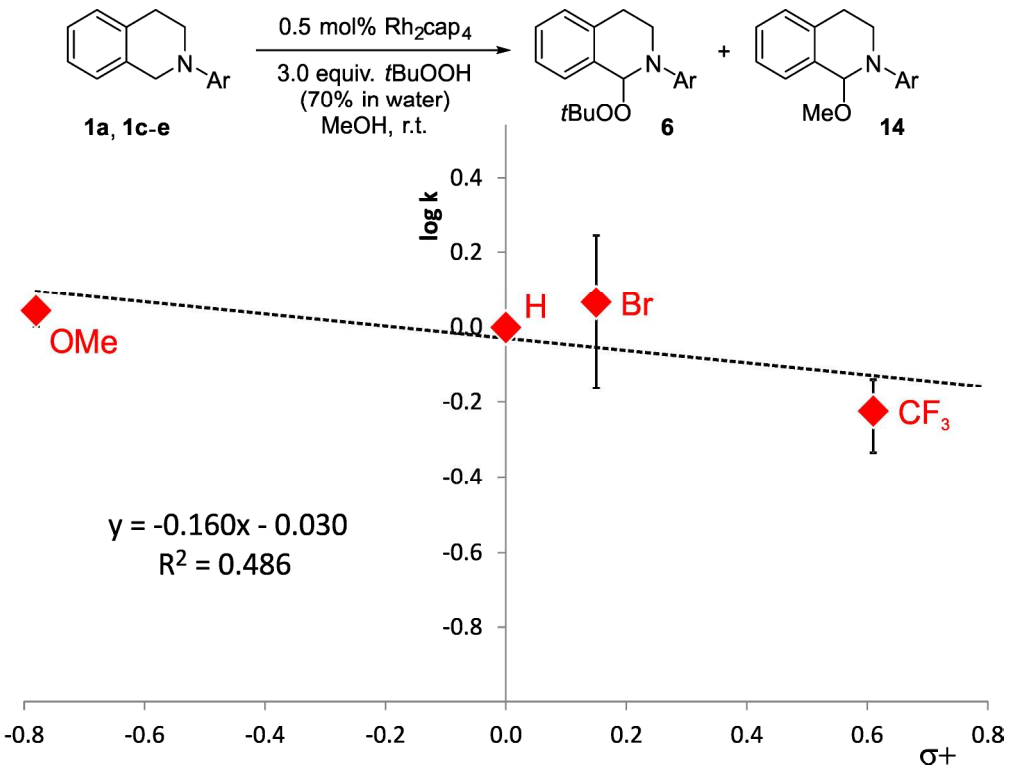

Figure 6
263x199mm (300 x 300 DPI)

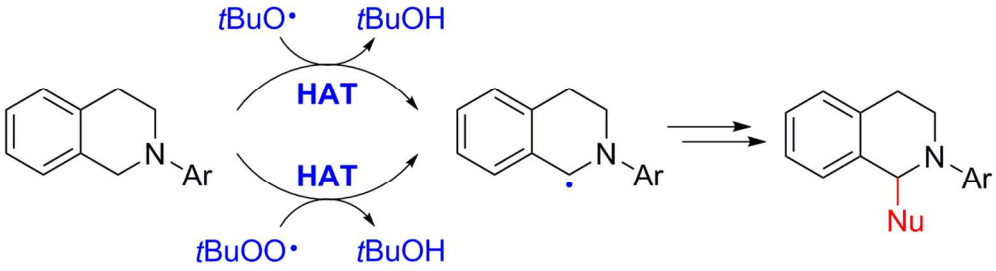

Table of Contents graphical abstract
117x33mm (300 x 300 DPI)